Statistics of Surface Layer Turbulence over the Tropical Ocean[1]

E. LEAVITT[2]

Dept. of Atmospheric Sciences, University of Washington, Seattle 98105

C. A. PAULSON

Dept. of Oceanography, Oregon State University, Corvallis 97331

(Manuscript received 6 June 1974, in revised form 10 September 1974)

ABSTRACT

Atmospheric surface layer turbulent statistics measured during the Barbados Oceanographic and Meteorological Experiment 8 and 30 m above mean sea level are presented. The budget equations of turbulent kinetic energy, humidity variance and temperature variance are examined. Within discussed limitations it is concluded that production equals dissipation in the case of turbulent kinetic energy and humidity variance. The analysis of the temperature variance budget revealed large differences between productions and dissipations computed assuming standard similarity functions derived from other data sets. Initial computation of fluxes revealed large systematic decreases with height in the shear stress and heat flux. Comparison with other results suggested corrections which would eliminate these differences. Comparison between profile fluxes and direct measurements suggests strong similarity of momentum and water vapor transfer.

1. Introduction

As part of a continuing investigation of the exchanges of momentum, heat and water between the atmosphere and the ocean surface the University of Washington participated in the Barbados Oceanographic and Meteorological Experiment (BOMEX). BOMEX is described by Kuettner and Holland (1969).

Observations were made aboard the research platform *Flip* during a two-week period, 2–13 May 1969, about 200 mi east of the island of Barbados. *Flip* is operated by the Marine Physical Laboratory of Scripps Institute of Oceanography. The fluctuations of wind, temperature and humidity, as well as the mean profiles of horizontal wind speed, temperature and humidity were measured. The computation of fluxes from the mean profiles has been reported in Paulson *et al.* (1972). This paper reports on an analysis of the statistics of the turbulent fluctuations. The budget equations of the turbulent fluctuations of wind, temperature and humidity have been examined in terms of similarity theory (Obukhov, 1946). Also fluxes of momentum, heat and water vapor have been computed from these data for comparison with those estimated from the profiles and by other investigators. Another paper reports on the spectral analysis of the data (Leavitt, 1975).

List of Symbols

g	acceleration due to gravity [$=9.78$ m s^{-2}]
k	von Kármán constant [$=0.4$]
ρ	density of moist air [$=1.15$ kg m^{-3}]
c_p	specific heat capacity of moist air [$=1030$ J kg^{-1} K^{-1}] corrected for moisture
L_E	heat of evaporation [$=2.42\times10^6$ J kg^{-1}]
u, v, w	longitudinal, lateral and vertical components of the wind
U	magnitude of mean horizontal wind
z	vertical coordinate
u_*	friction velocity [$=(\tau/\rho)^{\frac{1}{2}}$]
τ	wind stress
T	mean air temperature
θ	potential temperature
$\bar{\theta}$	mean potential temperature
θ_v	virtual potential temperature [$=\theta(1+0.61\,q)$]
q	specific humidity
Q	mean specific humidity
H	flux density of sensible heat [$=\rho c_p\overline{w\theta}$]
E	flux density of latent heat [$=\rho L_E\overline{wq}$]
θ_*	scaling temperature [$=-H/\rho c_p u_*$]
q_*	scaling humidity [$=-E/\rho L_E u_*$]
ϵ	dissipation of turbulent kinetic energy
N_θ	dissipation of temperature variance [$=\overline{\theta^2}/2$]
N_q	dissipation of humidity variance [$=\overline{q^2}/2$]
L	Monin-Obukhov scaling length corrected for humidity contribution to buoyancy {$=-T_v u_*^3/[\mathrm{kg}(\overline{w\theta}+0.61\,T\overline{wq})]$}
T_v	mean virtual temperature
n	frequency in hertz
κ	radian wavenumber

2. Data collection and analysis

The observational program on *Flip* was a cooperative one involving scientists from several institutions. Fig. 1

[1] Contribution No. 307, Department of Atmospheric Sciences, University of Washington.

[2] Present affiliation: AIDJEX, University of Washington.

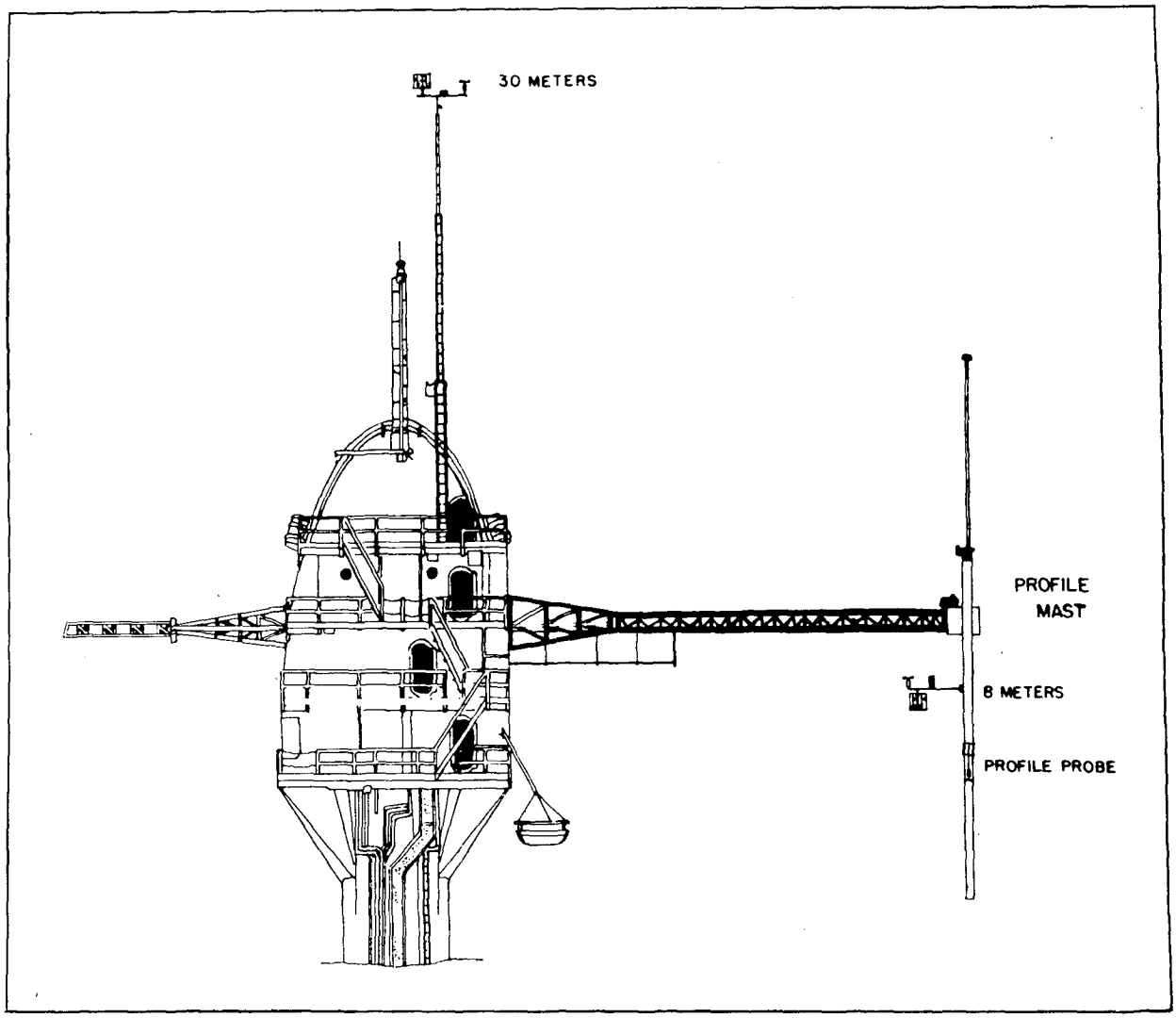

FIG. 1. Diagram of *Flip* showing the experimental arrangement.

shows the experimental arrangement. Turbulence measurements were made at two heights, 8 and 30 m above mean sea level. The three components of the wind field were measured at the two levels using similar Kaijo-Denki Company 3-D sonic anemometers. The anemometer at the 8 m level was operated by the University of British Columbia and the upper sonic by the University of Washington. Temperature and specific humidity fluctuations were measured at both heights with wet and dry thermocouples manufactured at the University of Washington. Oregon State University also measured temperature and humidity fluctuations at the lower level with a platinum resistance wire and a lyman-alpha humidiometer. An x-y-z accelerometer was used to measure ship's motions at the 30 m level and *Flip's* compass heading was monitored continuously. The University of California and Oregon State University measured wave heights with resistance wave gauges.

The data were originally recorded in analogue form on magnetic tape, each tape being about 45 min long. The data tapes were converted to digital form using a sampling rate which varied between 20 and 25 Hz. Aliasing was prevented by low-pass filtering of the data before digitizing. Preparing the digitized data for analysis included computation of the three wind components from the sonic anemometer; this involved correcting for mean vertical tilt and correcting for *Flip's* rotation about its vertical axis, and computation of the specific humidity variations from the wet and dry thermocouple outputs using the psychrometric equation. This data set was then used to compute Fourier spectra using a fast Fourier transform routine. These spectra were corrected for *Flip's* motion and for the fall-off in response of the temperature sensors as discussed below. A complete description of the analysis procedures can be found in Leavitt (1973). Covariances and variances were

computed for each 45-min period from the corrected spectra. Data from the 30 m level on 23 tapes have been analyzed as have data from the 8 m level on 17 of these tapes.

a. *Wind measurement corrections*

A description of the use of sonic anemometers and their limitations is found in Kaimal *et al.* (1968). It is critical to flux computations that the vertical alignment of the sonic anemometer be accurately known. For sufficiently long measuring periods the vertical velocity can be assumed to have zero mean; any vertical tilt can be determined from the measured mean horizontal and vertical velocities and a correction can be made. This procedure was used to compute the rotation angle required to correct the alignment of the 30 m sonic. Because of uncertainty in the measurement of the mean vertical velocity the rotation angles used were averages over several adjacent runs. A correction of 5.5° was applied to runs 60 to 77 inclusive but no correction was needed for runs 136 to 180 (Table 1). During the analysis of the 8 m data Pond *et al.* (1971) found a large error in the orientation of the 8 m sonic with respect to the mean wind. Unfortunately, the mean vertical velocity could not be determined due to an unknown electronic bias in the w channel. Their correction procedure assumed that the u and w fluctuations have a -0.5 correlation in the dimensionless frequency range $0.01 < nz/U < 0.1$ and each run was corrected separately by rotating the sonic velocities until the correlation

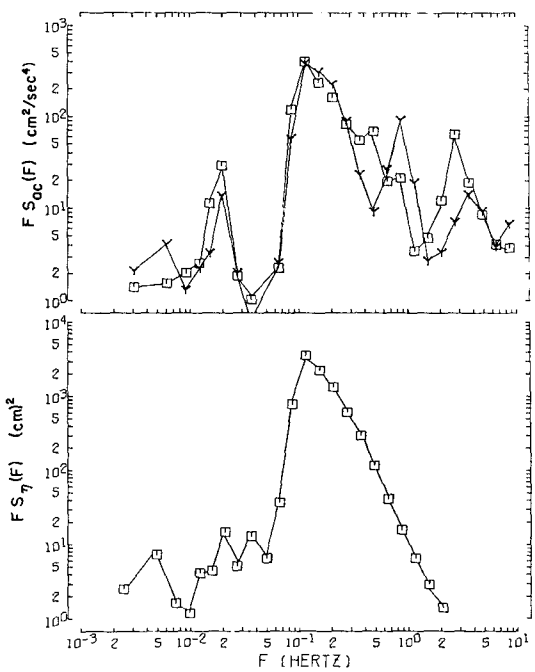

FIG. 2. Spectra of *Flip's* pitch (Y) and roll (⊡) accelerations as measured at 30 m (upper) and spectra from the University of California wave gauge for the same period (lower).

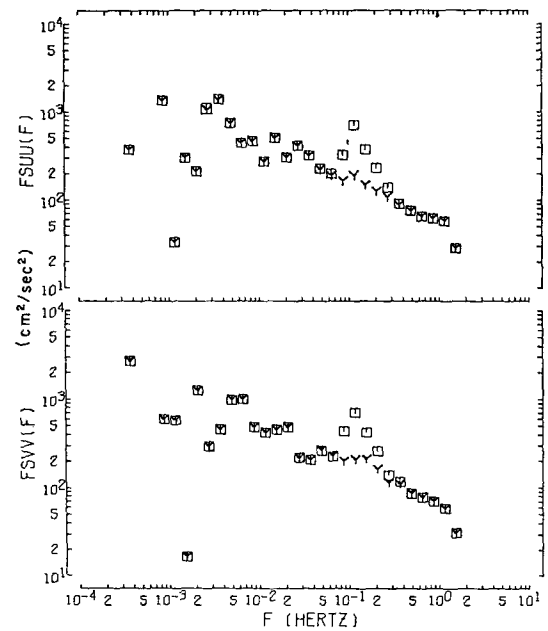

FIG. 3. Example of 30 m horizontal wind spectra (from run 181) corrected for ship's motion (Y) and uncorrected (⊡).

between u and w was -0.5 in this frequency band. The approach adopted in this paper was to look at this frequency range for groups of tapes and determine a single rotation angle for each group. This involved looking for the -0.5 correlation as well as trying to minimize the very low frequency components of the uw cospectra ($n < 10^{-3}$ Hz). Two rotation angles were necessary, $-10°$ for runs 60 to 77 and $-10.5°$ for runs 136 to 174. Pond *et al.* estimate the uncertainty in the stress measurements to be $\pm 20\%$ and in the heat flux and humidity measurements to be $\pm 10\%$. This corresponds to an uncertainty of $\pm 1.5°$ in the vertical orientation angle.

b. *Flip's motion*

An x-y-z accelerometer was positioned at the upper level and sample spectra of the pitch and roll motions as well as a wave height spectra are shown in Fig. 2. The results are similar to those of Rudnick (1967). The vertical accelerations are less than 1% of the horizontal accelerations and can be neglected. There is a large peak centered at 0.1 Hz and a smaller peak at 0.03 Hz. This latter peak is *Flip's* resonance frequency (Rudnick, 1967) and does not noticeably affect the velocity measurements. The motion at 0.1 Hz is reflected in a peak in the u and v spectra at 30 m and in all three 8 m velocity spectra. Because of its location on the side mast the lower sonic moved vertically when *Flip* rolled (Fig. 1). The integrated accelerometer spectra were used to correct the 30 m wind spectra for two data sets (Fig. 3). Because of malfunction of the accelerometers this procedure could not be followed for all data sets. In this

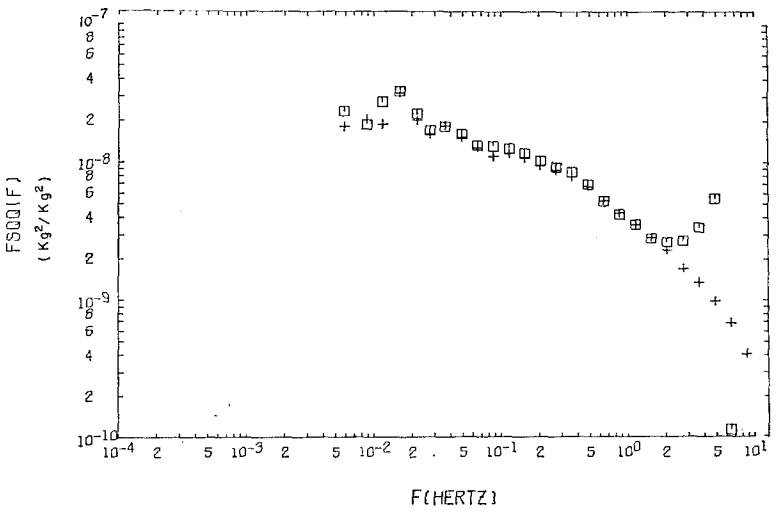

FIG. 4. Comparison between humidity spectra computed from the signals of the Oregon State University lyman-alpha (+) and the corrected thermocouple (⊡).

analysis corrections were made by drawing straight lines through the frequency band 0.08 to 0.2 Hz of the affected spectra.

Flip also rotated about its vertical axis in response to wind and current forces. This rotation had a variable period of 2 to 10 min and an extremely variable amplitude. The recorded ship's heading was used to correct the horizontal wind components for runs 136 through 180. Due to noise in this record corrections could not be made for runs 60 through 77. However, comparisons

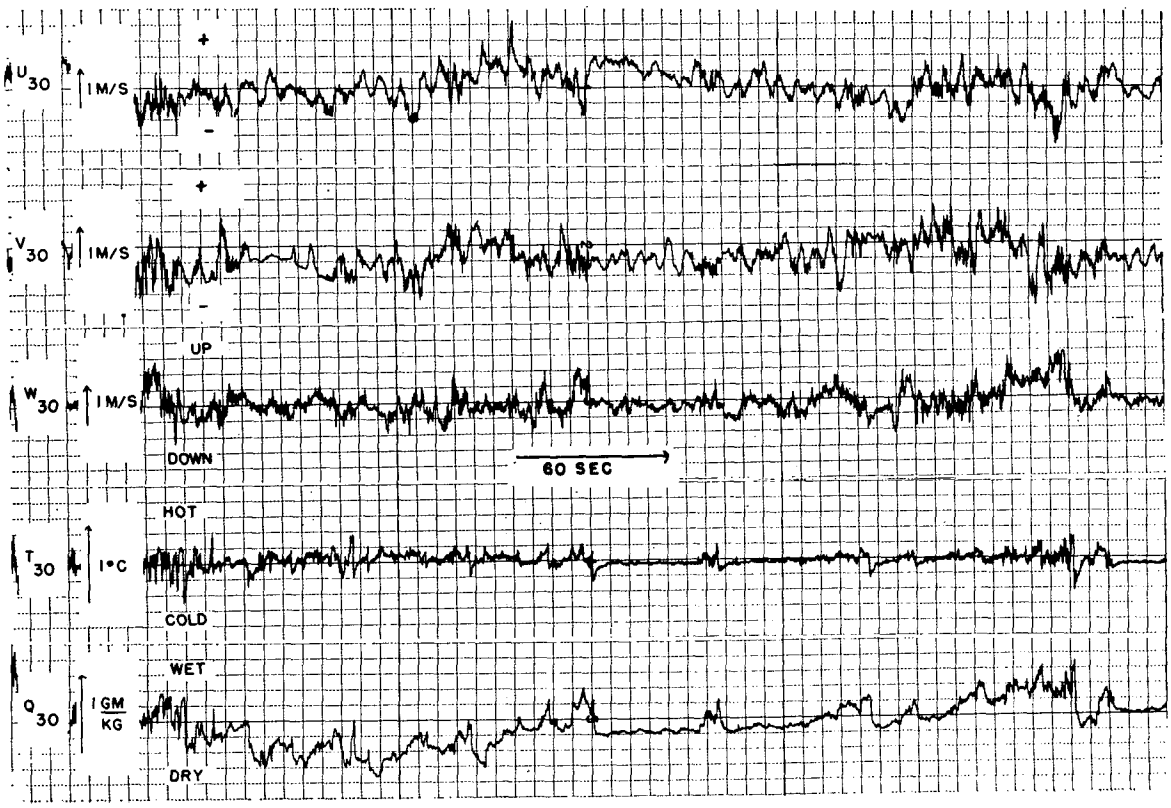

FIG. 5. Traces of u, v, w, T and q from 30 m, run 142. There are 6 min of continuous data.

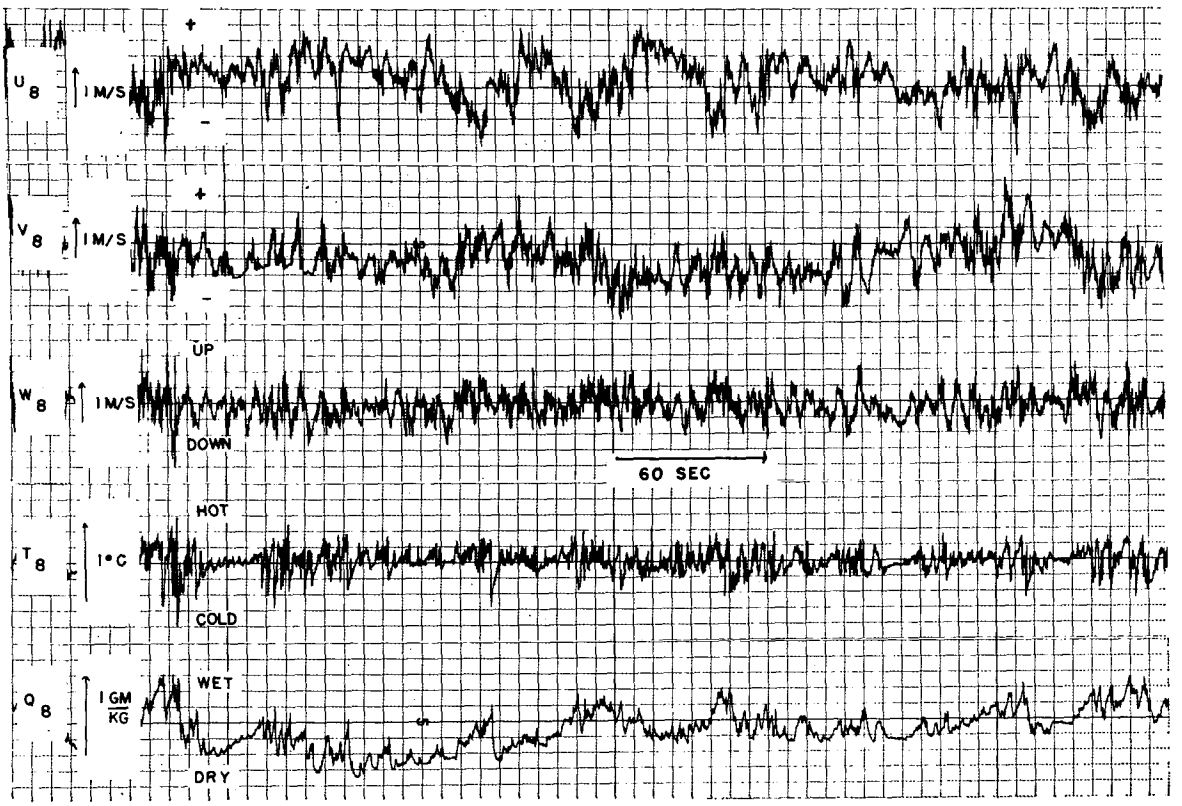

FIG. 6. Traces of u, v, w, T and q from 8 m, run 142. These data are concurrent with those shown in Fig. 5.

between corrected and uncorrected data show that any resultant error is small and is only important in considering low-frequency v fluctuations.

c. Temperature and humidity measurements

The thermocouples were copper-constantan pairs made with 3 mil wire. Moisture was supplied to the wet junction by a cotton thread which is wrapped around the junction. Specific humidity is computed from the measured wet and dry temperatures by use of the psychrometric equation

$$q=q_s(T_w)-c_pL_E^{-1}(T_w-T), \quad (1)$$

where T and T_w are the dry and wet temperatures and q_s the saturation specific humidity at temperature T_w. To extend the useful frequency bandwidth of the thermocouples a correction was applied to the high-frequency spectra assuming the thermocouples to be first-order low-pass filters. This filter has the spectral correction function

$$c(f)=1-jn/n_0. \quad (2)$$

Here $j=\sqrt{-1}$ and n_0 is the frequency at which the power is attenuated by 0.5 and the phase shift is 45°. The calculated frequency constants were 3 Hz for both dry thermocouples, 2 Hz for the 30 m wet sensor and 0.7 Hz for the 8 m wet sensor. Because of amplifier noise the correction is valid only for frequencies <5 Hz except for the 8 m wet sensor which is limited to frequencies <2 Hz.

Fig. 4 shows a comparison between humidity spectra computed from the 8 m thermocouple signals and the lyman-alpha. For frequencies <2 Hz the agreement is very good. However, the calibration constant computed for the lyman-alpha by matching the low-frequency components of the two instruments is about 30% less than the calibration constant that Pond *et al.* (1971) used in their analysis. This discrepancy will be referred to in a later section.

3. Time variations

a. Mean variations

Compared to most land sites the BOMEX area was smooth and homogeneous with small variations in wind speed, temperature and humidity during the two weeks of the experiment. The range of mean air temperature at 11 m above mean sea level was 27.5±0.6C and the variation in the bucket sea temperature was 28.2±0.3C. Most of the variation in sea temperature was in response to the diurnal variation in solar radiation. The mean specific humidity and mean wind speeds varied over a relatively wider range of values—0.015 to 0.018 kg kg^{-1}

TABLE 1. Tabulation of the direct flux measurements. Additional information is contained in Table 6.

Tape No.	Z/L 8M	Z/L 30M	-L 8M (meters)	-L 30M (meters)	Stress 8M N/m^2	Stress 30M N/m^2	H 8M W/m^2	H 30M W/m^2	E 8M W/m^2	E 30M W/m^2
60	-.11	-.64	70	44	.081	.051	16	11	104	99
62	-.25	-.75	33	38	.054	.051	20	14	99	118
63	-.10	-.71	78	40	.094	.058	18	13	127	163
64	-.13	-1.07	60	26	.078	.040	19	14	103	110
69	-.12	-.77	70	37	.095	.059	21	22	134	87
76	-.16	-1.60	50	18	.057	.031	12	15	103	104
77	-.25	-1.48	32	19	.031	.028	8	12	64	80
136	-.35	-.91	24	31	.038	.047	16	17	93	88
137	-.19	-.96	42	29	.057	.040	16	12	105	111
138	-.25	-1.22	32	23	.045	.027	15	8	93	82
139	-.28	-1.68	29	17	.040	.022	15	9	69	72
140	-.26	-1.75	31	16	.042	.020	13	4	90	115
141	-.19	-.79	43	36	.063	.052	19	15	99	125
142	-.27	-1.38	30	20	.048	.029	19	11	91	93
170	-.12	-.67	69	42	.089	.055	17	13	144	124
171		-1.59		18		.034		15		134
172	-.11	-.64	75	44	.077	.048	12	10	120	100
173	-.17	-1.34	46	21	.053	.028	11	9	109	93
174		-1.55		18		.031		12		120
177		-1.09		26		.054		26		120
178		-.78		36		.055		16		137
179		-.97		29		.050		19		126
180		-.79		36		.051		16		100

and 2.5 to 8.0 m s^{-1}, respectively. However, the mean wind speeds of the runs selected for analysis varied only between 4.5 and 8.0 m s^{-1}. A discussion of the diurnal variations in the data is contained in Paulson *et al.* (1972). The variation in stabilities for the runs analyzed was also small. At the 8 m level $-0.14 > z/L > -0.3$ and at 30 m $-0.45 > z/L > -1.5$. Approximately 40–50% of each z/L value is contributed by the water vapor flux.

Holland (1972) describes the averaged mean boundary layer profiles observed during the experiment. The potential temperature decreases with height to about 60 m and is then approximately constant to about 600 m where it begins to increase rapidly. The specific humidity decreases with height throughout the boundary layer, the decrease being less between 50 and 400 m. The mean horizontal wind speed increases with height up to the inversion level.

b. *Time series*

The data shown in Fig. 5 represent traces of the u, v, w, T and q fluctuations at 30 m for a continuous 6-min period from run 142. Fig. 6 shows the 8 m level traces for the same time period. The humidity trace looks very similar to the temperature trace seen in land data of unstable conditions: ramp-like positive excursions with a slow rise to a maximum departure from the mean value and then a sharp fall-off to slightly below the mean values. These ramps are associated with upward w and negative u variations while the v traces exhibit variations of either sign.

However, the BOMEX temperature signal is not typical. The passage of a humidity ramp is associated not only with the warmest temperatures but also with the coldest temperatures. The coldest temperatures occur when the humidity sharply decreases from a local maximum value at the upwind side of a ramp. This phenomenon was reported by Pond *et al.* (1971) who referred to these variations as cold spikes. During periods of minimum q the fluctuations of the five variables are very small. This is most noticeable in the u and v traces. The sinusoidal oscillations during these periods are due to *Flip's* motion. It can also be noted that there are no cold spikes during the quiescent periods.

4. Results

a. *Fluxes*

The measured fluxes are listed in Table 1 and additional statistics are tabulated in Table 6 (see Appendix). As described above the fluxes have been computed by integrating the appropriate frequency cospectra which is equivalent to Reynold's averaging.

Except for one run, 136, the measured shear stress is greater at 8 m than at 30 m. The mean stress decreases from 0.06 N m^{-2} at 8 m to 0.04 N m^{-2} at 30 m and the standard deviation of the difference is 0.013 N m^{-2}. The mean heat flux also decreases with height, from 15.8 W m^{-2} at 8 m to 12.3 W m^{-2} at 30 m. This decrease is not as consistent as the decrease in shear stress with the standard deviation of the difference, 3.94 W m^{-2}, being greater than the average difference, 3.49 W m^{-2}. In contrast to these differences the mean latent heat flux is 101 W m^{-2} at 8 m and 103 W m^{-2} at 30 m, a mean difference of only 2 W m^{-2}. The standard deviation of this difference is 9.8 W m^{-2}.

The vertical gradient of shear stress in the surface layer under stationary conditions depends on the pressure gradient in the direction of the mean flow. The pressure gradient required to balance the measured vertical shear stress gradient is 10 mb (1000 km)$^{-1}$. Such a large pressure gradient is unrealistic and would require the flow to be almost totally cross-isobaric. The results of an analysis of the BOMEX array momentum budget for the period 22–29 June 1969 (Holland and Rasmussen, 1971) were that the surface stress was 0.065 N m^{-2} and the rate of vertical decrease 0.01 N m^{-2} (100 m)$^{-1}$. Their calculated vertical gradient of shear stress would require a pressure gradient of only 1 mb (1000 km)$^{-1}$ in the x direction which is believed to be of the correct magnitude. Although the two measuring periods are not coincident there is no evidence of any large change in the air flow pattern between the two periods.

In a similar fashion the observed decrease in heat flux can be shown to be unrealistic. Neglecting molecular heat conduction the heat equation can be written as (Lumley and Panofsky, 1965)

$$\rho c_p \partial \ln\tilde{\theta}/\partial t = -\partial(H+R)/\partial z. \quad (3)$$

Since the left-hand side of (3) is small, it can be neglected; thus the equation can be written as a balance between the divergence of sensible heat and radiant fluxes. Following Funk (1961) the divergence in the radiative flux between 8 and 30 m was computed numerically to be less than 0.2 ± 0.2 W m^{-2}. The measured change in H with height is seen to be at least an order of magnitude too large.

Several reasons for the differences in fluxes at the 8 and 30 m levels can be advanced. It is possible that the averaging period (45 min) is not long enough to include all the frequencies that contribute to the fluxes. However, as is shown in Leavitt (1975) the mean error from this effect is expected to be less than 5% for the shear stress and less than 1% for the heat flux. A second source of systematic error would be the orientation of the sonics. The difference in the mean stress could be removed by a combined rotation of about 5°. However, such a correction would increase the difference between the sensible heat fluxes and introduce a systematic difference in the latent heat flux. A third source of error is in the calibrations of the instruments. As already mentioned the 8 m thermocouple humidity fluctuation amplitudes did not agree with those of the lyman-alpha humidiometer although the normalized humidity spectra agreed very well. In contrast the 8 m temperature spectra from the thermocouple and the Oregon State University platinum resistance wire thermometer agreed very well. This problem will be discussed further during the comparison with other experimental results. It will be concluded that the differences are probably due to calibration errors and correction factors will be suggested. These errors do not affect any comparison of properly nondimensionalized quantities from both heights.

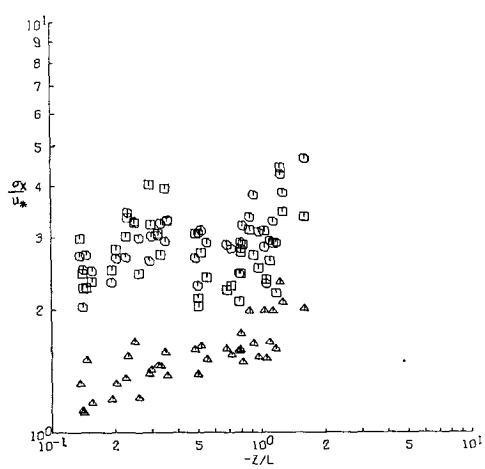

FIG. 7. Values of $\sigma_u/u_*(\boxdot)$, $\sigma_v/u_*(\odot)$ and $\sigma_w/u_*(\triangle)$ plotted against $-z/L$.

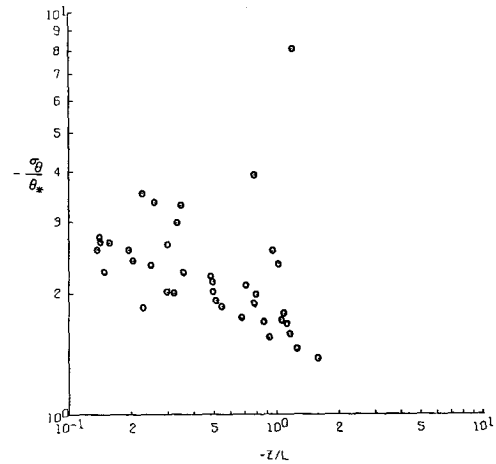

FIG. 8. Values of σ_θ/θ_* plotted against $-z/L$.

b. Variation of the turbulent fluctuations with stability

The ratios σ_w/u_*, σ_u/u_* and σ_v/u_* are plotted against $-z/L$ in Fig. 7. Because of the differences discussed above, the L values were computed by averaging the flux values from both heights for each run. The u_* used to nondimensionalize is the value from each height. Free convection arguments lead to a prediction that

$$\sigma_w/u_* = C_w(-z/L)^{\frac{1}{3}} \quad \text{for } z/L < -1.0, \quad (4)$$

where C_w is a constant. In a neutral atmosphere where height can be neglected it is also predicted that

$$\sigma_w/u_* = C_{wN}, \quad (5)$$

where C_{wN} is also a constant. The stability range of this data is restricted and Fig. 7 only suggests that σ_w/u_* could be approaching a slope of $\frac{1}{3}$ at $z/L < -1.0$

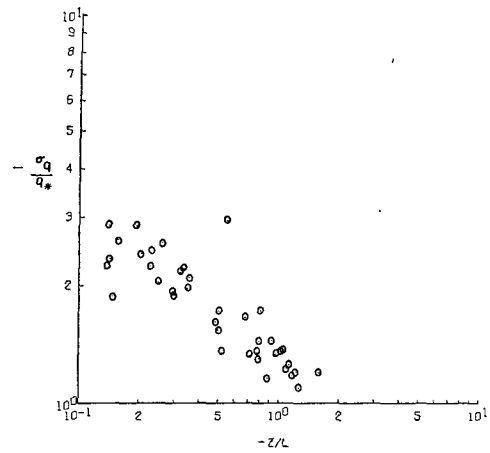

FIG. 9. Values of σ_q/q_* plotted against $-z/L$.

with $1.4<C_w<2.1$. C_{wN} is difficult to estimate because $z/L<-0.1$ but the trend of these data suggests a value between 1.1 and 1.3. Wyngaard and Coté (1971) estimate $C_w=1.9$ and $C_{wN}=1.2$ from data taken over wheat stubble in Kansas. Monji (1972) estimated $C_w=2.2$ and $C_{wN}=1.2$ from data taken on the Bonneville Salt Flats in Utah.

The σ_u/u_* and σ_v/u_* values are twice as large as σ_w/u_*. The σ_v/u_* ratio is constant in the stability range studied whereas the σ_u/u_* ratio shows a slight decrease with increasing instability. Since the u and v spectra show significant energy in the low frequencies it is possible that σ_u/u_* is being underestimated at the 30 m level. If the ratios are assumed constant at small values of $-z/L$ then the neutral values of σ_u/u_* and σ_v/u_* are both about 3.

The ratios σ_θ/θ_* and σ_q/q_* are plotted against $-z/L$ in Figs. 8 and 9, respectively. Similarity arguments can be used to predict that in free convection

$$-\sigma_\theta/\theta_*=C_\theta(-z/L)^{-\frac{1}{3}}, \quad (6)$$

$$-\sigma_q/q_*=C_q(-z/L)^{-\frac{1}{3}}, \quad (7)$$

where C_θ and C_q should be universal constants. The σ_θ/θ_* values do not exhibit a $-\frac{1}{3}$ region in the stability range of the data; the slope is about $-\frac{1}{4}$. The slope of $-\sigma_q/q_*$ is approximately $-\frac{1}{3}$. There is more scatter in the σ_θ results than in the σ_q results, as a result of occasional large variations in the low-frequency temperature spectra (Leavitt, 1975). Generally the $-\sigma_\theta/\theta_*$ values are greater than those observed in the Kansas and Utah experiments over the same stability range. Assuming a $-\frac{1}{3}$ slope C_q is 1.2 ± 0.4. Smedman-Högström (1973) also reported a value of 1.2 from data taken over land near Uppsala, Sweden.

c. *Kinetic energy budget*

Under stationary and horizontally homogeneous conditions the budget of turbulent kinetic energy can be written as (Lumley and Panofsky, 1965)

$$\overline{uw}\partial U/\partial z-(g/T_v)\overline{w\theta_v}+\partial(\overline{wu_i^2}/2)/\partial z+\epsilon+\rho^{-1}\partial\overline{pw}/\partial z=0. \quad (8)$$

This equation can be nondimensionalized by multiplying by $-kz/u_*^3$ to obtain

$$\Phi_m-z/L-D_u-\Phi_\epsilon-P_u=0. \quad (9)$$

Here $\Phi_m=(kz/u_*)\,\partial U/\partial z$ is the shear production, z/L is the buoyancy production including the affect of the humidity fluctuations, $D_u=(kz/u^{3*})\partial(\overline{wu_i^2}/2)/\partial z$ is the divergence in the vertical flux of the kinetic energy, $\Phi_\epsilon=kz\epsilon/u_*^3$ is the dissipation, and $P_u=(kz/u_*^3\rho^{-1})\partial\overline{pw}/\partial z$ is the transfer of energy from point to point by the pressure fluctuations.

According to Kolmorgoroff's law the one-dimensional u spectra in the inertial subrange can be written as

$$S_u(\kappa_1)=\alpha_u\epsilon^{\frac{2}{3}}\kappa_1^{-5/3}, \quad (10)$$

where $S_u(\kappa_1)$ is the spectral density at wavenumber κ_1, and α_u is a universal constant. Using Taylor's hypothesis [$(\kappa_1=2\pi n/U)$ where n is frequency and U is mean wind speed], Eq. (10) can be rewritten as

$$\Phi_\epsilon=[nS_u(n)/\alpha_u]^{\frac{2}{3}}(2\pi n/U)kz/u_*^3. \quad (11)$$

Eq. (11) was used to compute Φ_ϵ from a best fit of the u spectra vs frequency in the band of frequencies where the three wind spectra exhibited a $-\frac{2}{3}$ slope. See Leavitt (1975) for further details. Following Wyngaard and Coté (1971) a value of $\alpha_u=0.53$ was arbitrarily selected. The dimensionless shear production is the dimensionless mean velocity gradient. For unstable conditions Businger *et al.* (1971) suggest $\Phi_m=(1-15z/L)^{-0.25}$ which is similar to $\Phi_m=(1-16z/L)^{-0.25}$ which was used to com-

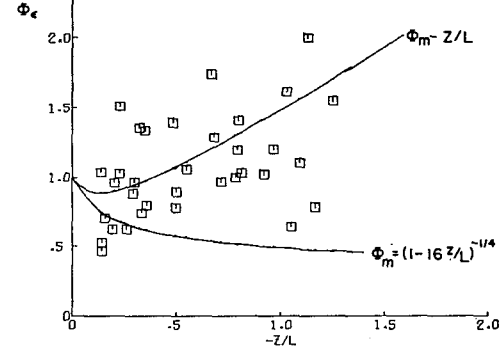

FIG. 10. The dimensionless dissipation [$\Phi_\epsilon=kz\epsilon/u_*^3$], dimensionless shear production [$\Phi_m=(1-16z/L)^{-\frac{1}{4}}$], and total dimensionless production [Φ_m-z/L] of the turbulent kinetic energy as a function of $-z/L$.

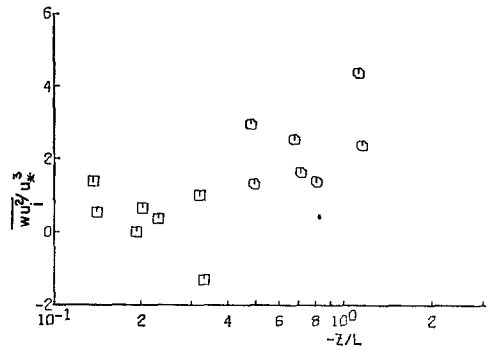

FIG. 11. The dimensionless turbulent kinetic energy flux $[\overline{wu_i^2}/u_*^3]$ as a function of $-z/L$: (⊡) 8 meter values, (⊙) 30 meter values.

pute shear stress from the *Flip* mean profiles by Paulson *et al.* (1972). The computed values of Φ_m according to this latter function are plotted vs z/L along with the measured dissipation values in Fig. 10. The scatter in Φ_ϵ is large but with the exception of a few 8 m data points the dissipation always exceeds the shear production. The total turbulent energy production by shear and buoyancy forces $(\Phi_m - z/L)$ is also compared to the dissipation values in Fig. 10. The total production is approximately equal to the dissipation. For comparison the mean dimensionless dissipation was 1.15 and the mean dimensionless total production was 1.22.

The divergence in the flux of turbulent kinetic energy (turbulent transport) can be approximated as

$$\partial(\overline{wu_i^2}/2)/\partial z = 0.5[\overline{wu_{i_{30}}^2} - \overline{wu_{i_8}^2}](z_8 z_{30})^{0.5}/\log(z_{30}/z_8), \quad (12)$$

where a logrithmic profile for the flux has been assumed between 8 and 30 m. Because the derivative could only be calculated at one height the range of observed stabilities is small. To accurately compute triple moments requires longer measuring periods than for the corresponding cospectra and all the uncertainties that must be accounted for in the flux results are compounded in these calculations. The turbulent transports were computed for seven 45-min periods in the time domain. Fig. 11, a plot of the dimensionless energy flux $\overline{wu_i^2}/u_*^3$ vs z/L illustrates the scatter in the measurements. Some of the kinetic energy fluxes at 8 m are negative although in unstable conditions they are expected to be positive. Consequently, the computed turbulent transports are probably overestimated. The turbulent transports are plotted vs z/L in Fig. 12. Wyngaard and Coté (1971) found the dimensionless transport to be approximately equal to z/L and the solid line in Fig. 12 follows this suggestion. However, the mean dimensionless transports for these estimates is only 0.2 whereas the mean value of $-z/L$ is 0.42.

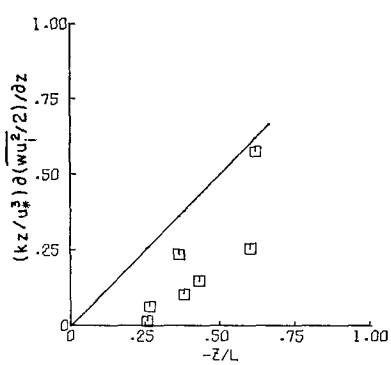

FIG. 12. The dimensionless turbulent energy transport $[D_u = (kz/u_*^3)\ \partial(\overline{wu_i^2}/2)/\partial z]$ as a function of $-z/L$. The solid line follows the suggestion of Wyngaard and Coté (1971) that $D_u = -z/L$.

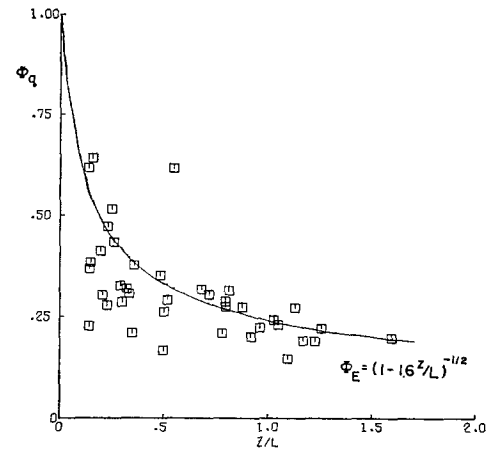

FIG. 13. The dimensionless rates of production $[\Phi_E = (1-16z/L)^{-\frac{1}{2}}]$ and dissipation $[\Phi_Q = kzN_Q/u_*q_*^2]$ of the humidity variance as a function of $-z/L$.

The pressure transport could not be measured and can only be inferred from the balance equation. If total production does equal dissipation as roughly suggested, then the turbulent transport is balanced by the pressure term. A similar imbalance was observed by Wyngaard and Coté, but the imbalance in these data is not significant because the cumulative uncertainties in the terms is of the same order as the imbalance.

d. Budget of the humidity variance

The specific humidity variance budget $(\overline{q^2}/2)$ can be written under stationary and homogeneous conditions as

$$\bar{w}\bar{q}\partial Q/\partial z + \partial(\overline{wq^2}/2)/\partial z + N_q = 0, \quad (13)$$

where N_q is the dissipation of the humidity variance.

Multiplying this equation by $-kz/u_*q_*^2$ gives the nondimensional form

$$\Phi_E - D_q - \Phi_q = 0, \quad (14)$$

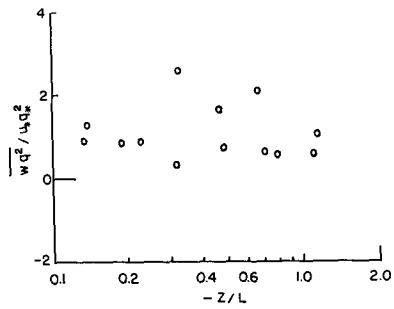

FIG. 14. The dimensionless humidity variance flux $[\overline{wq^2}/u_*q_*^2]$ as a function of $-z/L$.

where Φ_E is the dimensionless production, Φ_q the dimensionless dissipation, and D_q the dimensionless turbulent transport. Following ideas first suggested by Corrsin (1951), the one-dimensional inertial subrange spectra of a scalar such as humidity can be written as

$$S_q(\kappa_1)=\beta_q\epsilon^{-\frac{1}{3}}N_q\kappa_1^{-5/3}, \tag{15}$$

where β_q is a universal constant.

Using Taylor's hypothesis the dimensionless dissipation can be written as

$$\Phi_q=[nS_q(n)/\beta_q]\epsilon^{\frac{1}{3}}(kz/u_*q_*^2)(2\pi n/U). \tag{16}$$

Paquin and Pond (1971) computed $\beta_q=0.8\pm0.2$ from their measurements of the humidity structure functions using *Flip* data. Smedman-Högström (1973) estimates $\beta_q=0.58\pm0.2$ from the Uppsala data assuming equality of production and dissipation. Dyer and Hicks (1970) found $\Phi_E=(1-16z/L)^{-\frac{1}{2}}$. Note that this means $\Phi_E=\Phi_m^2$ (see previous section), and this function was used in computing fluxes from the mean profiles. The values of Φ_E and Φ_q using the above function for Φ_E and assuming $\beta_q=0.8$ are plotted vs z/L in Fig. 13. The 8 m dissipation values seem to be slightly lower than the corresponding Φ_E values but the 30 m values agree very well. The mean values for the data were $\Phi_q=0.32$ and $\Phi_E=0.34$.

The dimensionless humidity variance flux is plotted vs z/L in Fig. 14 and the dimensionless humidity transport calculated in the same manner as the kinetic energy transport is shown in Fig. 15. The mean transport is approximately 10% of the mean production, $\bar{D}_q=0.05$ and $\bar{\Phi}_q=0.37$. The scatter in D_q is very large and very little can be deduced about its behavior. Most of this scatter is probably due to the averaging period being too short.

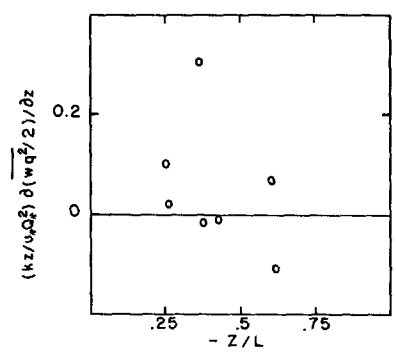

FIG. 15. The dimensionless transport of the humidity variance as a function of $-z/L$.

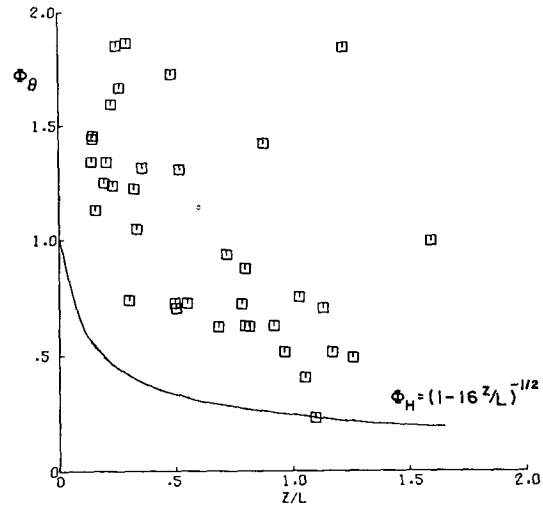

FIG. 16. The dimensionless rates of production $[\Phi_H=(1-16z/L)^{-\frac{1}{2}}]$ and dissipation $[\Phi_\theta=kzN_T/u_*\theta_*^2]$ of the temperature variance as a function of $-z/L$.

e. *Budget of temperature variance*

The budget of temperature variance $(\overline{\theta^2}/2)$ can be written as

$$\overline{w\theta}\partial\bar{\theta}/\partial z+\partial(\overline{w\theta^2}/2)/\partial z+N_\theta=0. \tag{17}$$

Multiplying this equation by $-kz/u_*\theta_*^2$ gives the dimensionless form

$$\Phi_H-D_\theta-\Phi_\theta=0, \tag{18}$$

where Φ_H is the dimensionless production, D_θ the dimensionless transport, and Φ_θ the dimensionless dissipation of $\overline{\theta^2}/2$. The relation $\Phi_H=(1-16z/L)^{-\frac{1}{2}}$ was used to compute the sensible heat flux from the mean profiles (Paulson *et al.*, 1972) and this function will be compared

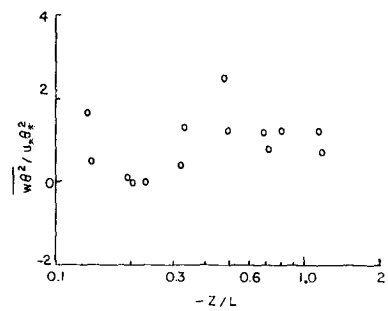

FIG. 17. The dimensionless temperature variance flux $[\overline{w\theta^2}/u_*\theta_*^2]$ as a function of $-z/L$.

to the dissipation estimates. The dimensionless dissipation of the temperature variance can be expressed in the same form as the expression for the humidity variance and is given by

$$\Phi_\theta = (nS_\theta(n)/\beta_\theta)(\epsilon^{-\frac{1}{3}}kz/u_*\theta_*^2)(2\pi n/U), \qquad (19)$$

where β_θ should be a universal constant but estimates in the literature vary widely. Recent measurements that assumed production equals dissipation indicate $\beta_\theta = 0.8$ (Wyngaard and Coté, 1971). However, two recent determinations of β_θ from direct measurements of N_θ indicate $\beta_\theta = 1.6$ (Boston and Burling, 1972) and $\beta_\theta = 2.0$ (Gibson *et al.*, 1970). This latter value was determined from *Flip* data taken during BOMEX and has been used to compute the dissipation values which are compared to $\Phi_H = (1-16z/L)^{-0.5}$ in Fig. 16. The computed Φ_θ and Φ_H values do not agree and the mean values are $\Phi_\theta = 1.21$ and $\Phi_H = 0.37$. If $\beta_\theta = 0.8$ were substituted in (19) the dissipation estimates would be 2.5 times larger and the disagreement would be even greater.

The dimensionless temperature variance flux $(\overline{w\theta^2}/u_*\theta_*^2)$ and the dimensionless temperature transport are plotted vs z/L in Figs. 17 and 18, respectively. The mean value of the transport was 0.09 which is about 25% of the corresponding mean value of Φ_H. The temperature transport shows considerably less scatter than the measurement of the humidity transport because most of the temperature variance is concentrated in frequencies above 10^{-2} Hz in contrast to humidity (Leavitt, 1975). The transport represents a loss in the stability range studied but the trend in the data indicates that it could become a gain at larger $-z/L$ values. This would be consistent with Deardorff's (1966) suggestion that the turbulent transport can support a countergradient heat flux. Wyngaard and Coté (1971) observed a similar behavior in their Kansas data.

f. Comparison with other BOMEX results

The Universities of British Columbia and Oregon State measured fluxes at the 8 m level. The results of their analyses are reported in Pond *et al.* (1971), Phelps and Pond (1971) and Paquin and Pond (1971). Several of their runs overlapped with the data presented in this paper. The flux measurements from these runs are compared in Table 2. The average stress and heat flux values agree well but the latent heat flux estimated using the thermocouples was 101 W m^{-2} as compared to 123 W m^{-2} estimated using the lyman-alpha, a difference of about 20%.

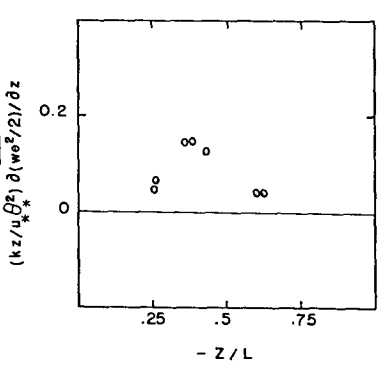

FIG. 18. The dimensionless transport of the temperature variance as a function of $-z/L$.

TABLE 2. Comparison of the direct flux measurements of Oregon State University (OSU) and the University of British Columbia (UBC) (Pond *et al.*, 1971) with those of the University of Washington (UW). All data are from the 8 m level.

Tape No. UW	Tape No. OSU	(Minutes) UW	(Minutes) OSU	Overlap (min)	Stress UW N/m^2	Stress OSU N/m^2	Heat Flux UW W/m^2	Heat Flux OSU W/m^2	Latent Heat Flux UW W/m^2	Latent Heat Flux OSU W/m^2
60	10	44	62	33	.081	.077	16	13	104	114
76		44		42	.057		12		103	
77	11	44	75	29	.031	.044	8	10	64	105

Tape No. UW	Tape No. UBC	(Minutes) UW	(Minutes) UBC	Overlap (min)	Stress UW N/m^2	Stress UBC N/m^2	Heat Flux UW W/m^2	Heat Flux UBC W/m^2	Latent Heat Flux UW W/m^2	Latent Heat Flux UBC W/m^2
69	1	44	43	43	.095	.078	21	18	134	198
76	3	44	42	42	.057	.049	12	13	103	131
77	4	44	28	28	.031	.044	8	9	64	90

The NOAA Research Flight Facility DC-6 instrumented with a gust probe system made airborne measurements of water vapor flux during BOMEX as described by Bean *et al.* (1972). Aircraft data from 11 May 1969, supplied by the CEDDA office in Washington, D. C., was used to compute latent heat fluxes. Table 3 compares four consecutive *Flip* runs and simultaneous aircraft flights. The aircraft flights were at three different heights between 18 and 150 m and were each of 10-min duration so there are differences in the sample spaces. The difference between the mean *Flip*

TABLE 3. Comparison of the University of Washington (UW) estimates of latent heat flux with NOAA Research Flight Facility DC-6 aircraft measurements. Each aircraft run is about 6 min long.

UW Tape No.	Latent Heat Flux UW 8M W/m^2	Latent Heat Flux UW 30M W/m^2	Latent Heat Flux RFF W/m^2	RFF Height meters	Flight Direction - Wind
136	93	88	101	160	UP Wind
			103	50	Down
			99	20	Up
			125	160	Cross
			116	50	Cross
137	105	111	100	20	Cross
			120	160	Up
			128	50	Down
			193	20	Up
138	93	82	157	160	Cross
			142	50	Cross
			137	20	Cross
			162	60	Up
			107	50	Down
139	69	72	112	20	Up
			118	160	Cross
			119	50	Cross
			105	20	Cross
Averages	90	88	125		

TABLE 4. Comparison of the directly measured fluxes from both heights with the corrected profile results (Paulson *et al.*, 1972).

Tape No.	Stress Profile N/m^2	Stress Direct Average	8M	30M	H Profiles W/m^2	H Direct Aver.	8M	30M	E Profiles W/m^2	E Direct Aver.	8M	30M
		N/m^2				W/m^2				W/m^2		
60	.062	.066	.081	.051	4	14	16	11	130	100	100	100
62	.065	.076	.094	.058	6	15	18	13	150	140	130	160
63	.062	.052	.054	.051	6	17	20	14	140	110	100	120
64	.067	.059	.078	.040	7	16	19	14	160	110	100	110
69	.087	.077	.095	.059	8	21	21	22	210	110	130	90
76	.056	.044	.057	.031	6	13	12	15	180	100	100	100
77	.034	.030	.031	.028	4	10	8	12	130	70	60	80
136	.047	.043	.038	.047	7	17	16	17	160	90	90	90
137	.072	.049	.057	.040	6	12	16	12	180	110	110	110
138	.060	.036	.045	.027	7	11	15	8	160	90	90	80
139	.049	.031	.040	.022	4	13	15	9	160	70	70	70
140	.061	.031	.042	.020	4	9	13	4	180	100	90	120
141	.070	.057	.063	.052	4	17	19	15	180	110	100	130
142	.082	.039	.048	.029	3	15	19	11	200	90	90	90
170	.090	.072	.089	.055	9	15	17	13	240	130	140	120
171	.076	-	-	.034	7	-	-	15	210	-	-	130
172	.089	.063	.077	.048	9	11	12	10	240	110	120	100
173	.072	.041	.053	.028	9	10	11	9	230	100	110	90
174	.057	-	-	.031	8			12	170	-	-	120
177	.073	-	-	.054	4			26	170	-	-	120
178	.068	-	-	.055	7			16	190	-	-	140
179	.086	-	-	.050	7			19	210	-	-	130
180	.089	-	-	.051	9			16	230	-	-	100
Averages*	.068	.050	.061	.040	6	14	16	12	180	102	101	103

*Average includes only runs for which both direct measurements are available.

flux and the aircraft flux is approximately 40%; thus it appears that the thermocouple latent heat fluxes are being underestimated by approximately 30%.

If a calibration correction is applied to the 8 m thermocouple increasing the estimated flux at that level, the mean water vapor flux will show a decrease with height of the same order as the shear stress and sensible heat flux. These differences would be essentially eliminated if the calibration of each channel of the 30 m sonic anemometer is increased about 15%. This would increase the estimated 10 m neutral drag coefficient from 0.95×10^{-3} to 1.1×10^{-3}. This latter value is in better agreement with other measurements over the open ocean as reported by Brocks and Krügermeyer (1970). The z/L values would change only slightly

TABLE 5. Comparison of the University of Washington (UW) dissipation estimates and direct flux measurements from run 76 with the results of Stegan *et al.* (1973).

DISSIPATION VALUES

UW z (m)	UW ϵ (m^2sec^{-3}) 10^4	UW N_θ ($°k^2sec^{-1}$) 10^4	UCSD z (m)	UCSD ϵ (m^2sec^{-3}) 10^4	UCSD N_θ ($°k^2sec^{-1}$) 10^4
28	4.3	0.03			
			11.69	8.6	0.3
8	23.9	3.38			
			6.70	25.6	1.01
			3.89	40.9	1.14
			2.39	63.1	2.74

FLUX VALUES

UW z (m)	UW τ $N\ m^{-2}$	UW H $W\ cm^{-2}$	UCSD z (m)	UCSD τ $N\ m^{-2}$	UCSD H $W\ m^{-2}$
28	.028	16.1			
			11.69	.030	8.9
8	.047	21.9			
			6.70	.044	12.3
			3.89	.043	9.0
			2.39	.041	9.9

because both u_* and the heat fluxes are increased and none of these suggested corrections would affect dimensionless results. The 8 m hygrometer probably gave a low reading because the wick supplied insufficient moisture to the thermocouple junction and the total wet bulb depression was not maintained. It is possible that this was true to a lesser extent for the 30 m hygrometer. Because the fluctuations in the wet temperature were about four times larger than the temperature fluctuations the phase relations between temperature and humidity were not appreciably affected by this error. The possibility that the sonic calibration was incorrect is suggested by the results of Tsvang *et al.* (1973) who found during a comparison of different sonic anemometers that the Kaijo-Denki internal calibration circuit can be in error.

Fluxes of momentum, heat and water vapor were computed from the mean profiles (Paulson *et al.*, 1972) by integrating (Paulson, 1970) the flux gradient relation described in the budget analyses sections. Because of anomalous profile curvature and anomalously low initial computed shear stresses, assumed due to structural interference with the mean flow by *Flip*, a correction was applied to the mean profiles. The correction procedure used a comparison between the computed profile stresses and the direct fluctuation measurements from Pond *et al.* (1971). Corrected and uncorrected profile fluxes are compared to the direct measurements in Table 4. The corrected profile stresses agree very well with the 8 m results, as expected since they were used to correct the profiles. If the corrections described above are applied to the 30 m data they would also agree with the profile results. The profile heat fluxes are considerably lower than the directly measured fluxes, the mean ratio being about 2.4. If the measured temperature profiles

are correct this implies $\Phi_H \approx 0.4(1-16z/L)^{-0.5}$. This correction would make the disagreement in the computed temperature variance budget even greater. In contrast to the sensible heat fluxes, the profile latent heat fluxes are greater than the directly measured values, the mean ratio being 1.80. If the calibration correction described above is applied this ratio is reduced to 1.4.

Another comparison can be made with the direct dissipation measurements from *Flip* reported by Stegen *et al.* (1973). They measured the dissipation of turbulent kinetic energy and of temperature variance at four heights between 2 and 12 m using fast response sensors mounted on the profile probe. In Table 5 their measurements are compared to dissipation values estimated from the spectral inertial subrange assuming $\alpha_u = 0.53$ and $\beta_\theta = 2.0$ (run 76). Stegen *et al.* determined $\alpha_u = 0.6$ and $\beta_\theta = 2.0$ from their measurements. The turbulent kinetic energy estimates agree very well but the temperature variance dissipation estimates are considerably different. Using equations deduced assuming production equals dissipation, the shear stress (τ) and sensible heat fluxes (H) computed from the dissipation estimates

$$\tau = \rho(kz\epsilon/\Phi_\epsilon)^{\frac{2}{3}}, \tag{20}$$

$$H = \rho c_p(kzu_* N_\theta/\Phi_\theta)^{0.5}, \tag{21}$$

are also listed in Table 5. Here it is assumed that $\Phi_\epsilon = \Phi_m - z/L$ and $\Phi_\theta = \Phi_H$.

The shear stress values are in good agreement with the direct measurements (Table 1) but the heat flux computed from the inertial subrange spectra is about twice as large as the other estimates. This was expected from the discussion of the temperature variance budget. However, the heat flux computed from the results of Stegen *et al.* agrees fairly well with the direct flux measurement. These differences can only be resolved by further measurement of temperature fluctuations under similar conditions.

5. Conclusions

The budget equation results show that within the limits of the assumptions the local production and dissipation of turbulent kinetic energy and the humidity variance are approximately equal, with turbulent diffusion being less than 15% of the total production. Comparison between direct measurements and profile flux measurements suggested that $\Phi_E \approx \Phi_m$ rather than Φ_m^2 in the stability range studied. A strong similarity between momentum transfer and humidity transfer was also suggested by the results of Pond *et al.* (1971) and by Leavitt (1975). If this suggestion is correct then β_q would be reduced from 0.8 to approximately 0.55. This latter value is in approximate agreement with the value of 0.58 reported by Smedman-Högström (1973).

The computed production and dissipation of temperature variance did not agree with each other. The transport term, which showed behavior similar to that observed by Wyngaard and Coté (1971), was not large enough to account for this difference. There was also disagreement between profile and direct flux measurements and between a direct estimation of the dissipation and an estimate assuming the existence of an inertial subrange. The comparison of the different flux measurements suggests that similarity theory may need modification. It is also apparent that the inertial subrange assumptions may not hold in at least some circumstances. These questions will be discussed further in Leavitt (1975) after presentation of the spectral results.

Acknowledgments. This work was supported by National Science Foundation under Grants GA-4091 and GA-1099. We would like to acknowledge the advice and support rendered by Dr. R. G. Fleagle and Dr. J. Businger. This paper was written while E. Leavitt was a NSF-supported research associate with the Civil Engineering Department of Stanford University.

APPENDIX

TABLE 6. Supplementary data from the University of Washington data analysis.

Tape No.	Time Day (May, 1969)	Time GMT	U 8M (m/s)	U 30M (m/s)	$-\overline{uw}$ 8M (m^2/s^2 (10^4))	$-\overline{uw}$ 30M (m^2/s^2 (10^4))	$\overline{wT}$ 8M (°C m/s [10^2])	$\overline{wT}$ 30M (°C m/s [10^2])	$\overline{wq}$ 8M (m/s [10^4])	$\overline{wq}$ 30M (m/s [10^4])
60	6	0346	6.50	7.00	701	441	1.34	.95	.375	.355
62	6	0536	6.50	7.00	820	501	1.72	1.14	.357	.423
63	6	0626	6.50	7.00	467	444	1.48	1.09	.457	.584
64	6	0720	6.50	7.00	676	347	1.56	1.17	.369	.393
69	6	1137	6.90	7.30	842	512	1.73	1.85	.48	.312
76	6	1810	5.50	5.90	492	271	1.00	1.24	.37	.375
77	6	1902	5.05	5.40	271	245	.66	1.03	.23	.286
136	11	1608	5.70	6.00	330	410	1.39	1.47	.335	.318
137	11	1725	6.80	7.10	499	350	1.36	.98	.377	.40
138	11	1816	5.90	6.20	394	234	1.25	.66	.333	.293
139	11	1922	5.50	5.80	348	192	1.26	.74	.248	.258
140	11	2019	6.20	6.50	362	176	1.10	.35	.325	.414
141	11	2125	6.70	7.00	543	452	1.60	1.24	.354	.449
142	11	2219	6.70	6.90	418	254	1.59	.91	.326	.335
170	13	0422	7.45	7.65	774	480	1.46	1.09	.518	.447
171	13	0515	7.30	7.70	-	292	-	1.29	-	.480
172	13	0608	7.50	7.90	672	414	1.0	.80	.430	.361
173	13	0700	6.60	7.00	462	243	.95	.78	.39	.334
174	13	0750	6.30	6.70	-	265	-	1.03	-	.43
177	13	1113	7.00	7.40	-	466	-	2.21	-	.43
178	13	1205	6.65	6.95	-	481	-	1.35	-	.492
179	13	1256	6.70	7.20	-	435	-	1.56	-	.454
180	13	1347	6.90	7.25	-	446	-	1.38	-	.358

TABLE 6. (*Continued*)

Tape No.	σ_u 8M	σ_u 30M	σ_v 8M	σ_v 30M	σ_w 8M	σ_w 30M	σ_T 8M	σ_T 30M	σ_Q 8M	σ_Q 30M
	m/s		m/s		m/s		c°		Gm/kg	
60	.742	.429	.663	.645	.296	.292	.14	.09	.33	.29
62	.726	.607	.747	.675	.334	.314	.15	.11	.41	.35
63	.702	.479	.581	.513	.325	.312	.14	.10	.46	.40
64	.650	.416	.607	.536	.314	.300	.15	.11	.41	.35
69	.672	.542	.713	.658	.339	.342	.16	.15	.44	.41
76	.543	.447	.662	.626	.27	.272	.15	.12	.43	.33
77	.449	.344	.534	.457	.240	.252	.12	.10	.31	.21
136	.585	.479	.547	.469	.259	.308	.16	.12	.35	.22
137	.675	.516	.60	.528	.304	.328	.21	.21	.38	.28
138	.801	.475	.522	.435	.277	.304	.17	.10	.32	.26
139	.614	.479	.617	.533	.258	.289	.15	.08	.28	.20
140	.751	.587	.558	.567	.300	.310	.19	.21	.34	.38
141	.653	.487	.620	.598	.307	.330	.17	.12	.37	.28
142	.626	.463	.619	.523	.299	.316	.16	.10	.35	.27
170[1]	.631	.602	.757	.683	-	.357	.12	.10	.35	.28
171	-	.576	-	.767	-	.344	.12	.10	.42	.34
172	.771	.624	.701	.544	.342	.326	.10	.09	.37	.29
173[1]	.701	.488	.706	.524		.310	.10	.09	.37	.25
174		.95		.65		.320		.11		.26
177		.568		.633		.359	.14	.18	.38	.25
178		.460		.537		.348	.12	.12	.39	.30
179		.528		.646		.320	.18	.19	.37	.29
180		.518		.615		.337	.12	.12	.38	.25

[1]High frequency noise on 8M w channel, σ_w could not be estimated correctly.

REFERENCES

Bean, B. R., R. Gilmer, R. L. Grossman and R. McGavin, 1972: An analysis of airborne measurements of vertical water vapor flux during BOMEX. *J. Atmos. Sci.*, **29**, 860–869.

Boston, E. J., and R. W. Burling, 1972: An investigation of high-wavenumber temperature and velocity spectra in air. *J. Fluid Mech.*, **55**, 473–492.

Brocks, K., and L. Krügermeyer, 1970: The hydrodynamic roughness of the sea surface. Berichte 14, Instituts fur Radiometeorologie and Maritime Meteorology der Universitat Hamburg.

Businger, J. A., J. C. Wyngaard, Y. Izumi and E. F. Bradley, 1971: Flux-profile relationships in the atmospheric surface layer. *J. Atmos. Sci.*, **28**, 181–189.

Corrsin, S., 1951: On the spectrum of isotropic temperature fluctuations in an isotropic turbulence. *J. Appl. Phys.*, **22**, 469–473.

Deardorff, J. W., 1966: The countergradient heat flux in the lower atmosphere and in the laboratory. *J. Atmos. Sci.*, **23**, 503–506.

Dyer, A. J., and B. B. Hicks, 1970: Flux gradient relationships in the constant flux layer. *Quart. J. Roy. Meteor. Soc.*, **96**, 715–721.

Funk, J. P., 1961: A numerical method for the computation of the radiative flux divergence near the ground. *J. Meteor.*, **18**, 388–392.

Gibson, C. H., G. R. Stegen and R. B. Williams, 1970: Statistics of the fine structure of turbulent velocity and temperature fields measured at high Reynolds number. *J. Fluid Mech.*, **41**, part 1, 153–167.

Holland, J. Z., 1972: Comparative evaluation of some BOMEX measurements of sea surface evaporation, energy flux and stress. *J. Phys. Oceanogr.*, **2**, 476–486.

——, and E. M. Rasmusson, 1971: Measurements of the atmospheric mass, energy and momentum budgets over a 500 km square of tropical ocean. Paper presented at Seventh Tech. Conf. on Hurricanes and Tropical Meteorology, Barbados, Amer. Meteor. Soc.

Kaimal, J. C., J. C. Wyngaard and D. A. Haugen, 1968: Deriving power spectra from a three-component sonic anemometer. *J. Appl. Meteor.*, **7**, 827–837.

Kuettner, J. P., and J. Holland, 1969: The BOMEX project. *Bull. Amer. Meteor. Soc.*, **50**, 394–402.

Leavitt, E., 1973: Spectral characteristics and statistics of surface layer turbulence over the tropical ocean, Ph.D. thesis, University of Washington, 163 pp.

——, 1975: Spectral characteristics of surface layer turbulence over the tropical ocean. *J. Phys. Oceanogr.*, **5**, 157–163.

Lumley, J. L., and H. A. Panofsky, 1964: *The Structure of Atmospheric Turbulence*. Interscience, 239 pp.

Monji, N., 1972: Budgets of turbulent energy and temperature variance in the transition zone from forced to free convection. Ph.D. thesis, University of Washington, 125 pp.

Obukhov, A. M., 1946: Turbulence in an atmosphere with a non-uniform temperature. Translation (1971): *Boundary Layer Meteor.*, **2**, 7–29.

Paquin, J. E., and S. Pond, 1971: The determination of the Kolmorgoroff constants for velocity, temperature and humidity fluctuations from second- and third-order structure functions. *J. Fluid Mech.*, **50**, part 2, 257–269.

Paulson, C. A., 1970: The mathematical representation of wind speed and temperature profiles in the unstable atmospheric surface layer. *J. Appl. Meteor.*, **9**, 857–861.

——, E. Leavitt and R. G. Fleagle, 1972: Air-sea transfer of momentum, heat and water determined from profile measurements during BOMEX. *J. Phys. Oceanogr.*, **2**, 487–497.

Phelps, G. T., and S. Pond, 1971: Spectra of the temperature and humidity fluctuations and of the fluxes of moisture and sensible heat in the marine boundary layer. *J. Atmos. Sci.*, **28**, 918–928.

Pond, S., G. T. Phelps, J. E. Paquin, G. McBean and R. W. Stewart, 1971: Measurements of the turbulent fluxes of momentum, moisture and sensible heat over the ocean. *J. Atmos. Sci.*, **28**, 901–917.

Rudnick, P., 1967: Motion of a large spar buoy in sea waves. *J. Ship Res.*, **11**, 257–277.

Smedman-Högström, A. S., 1973: Temperature and humidity spectra in the atmospheric surface layer. *Boundary Layer Meteor.*, **3**, 329–347.

Stegen, G. R., C. M. Gibson and C. A. Friehe, 1973: Measurements of momentum and sensible heat fluxes over the open ocean. *J. Phys. Oceanogr.*, **3**, 86–92.

Tsvang, L. R., B. M. Koprov, S. L. Zubkovskii, A. J. Dyer, B. Hicks, M. Miyake, R. W. Stewart and J. W. McDonald, 1973: A comparison of turbulence measurements by different instruments, Tsimiyansk Field Experiment 1970. *Boundary Layer Meteor.*, **3**, 499–521.

Wyngaard, J. C., and O. R. Coté, 1971: The budgets of turbulent kinetic energy and temperature variance in the atmospheric surface layer. *J. Atmos. Sci.*, **28**, 190–201.